Journal of the Korean Chemical Society
2015, *Vol. 59, No. 5*
Printed in the Republic of Korea
http://dx.doi.org/10.5012/jkcs.2015.59.5.423

Effects of Binary Doping on Chiroptical, Electrochemical, and Morphological Properties of Chiral Polyaniline

Eunok Kim
Department of Chemistry, The University of Suwon, Hwaseong-si, Gyeonggi-do 445-743, Korea
E-mail: eokim@suwon.ac.kr
(Received July 2, 2015; Accepted July 9, 2015)

ABSTRACT. (1*S*)-(+)-10-camphorsulfonic acid (CSA) and HCl were used together as a binary dopant in the electrodeposition of polyaniline (PAni). (+)-CSA and HCl were added in different mole ratios (9:1 and 6:4). (+)-CSA-doped and binary-doped PAni exhibited markedly different ultraviolet-visible and circular dichroism spectral characteristics due to differences in their conformations. Distinct helical structures are observed in the scanning electron microscopy images of (+)-CSA-doped PAni. The X-ray diffraction pattern of (+)-CSA-doped PAni exhibited remarkably higher crystallinity than that of HCl-doped PAni which is associated with the helical ordering along the polymer chains. The conformational changes due to the binary doping in chiral PAni had a significant effect on its chiroptical and electrochemical properties, morphology, and crystallinity, thus determined its conductivity.

Key words: Conducting polymers, Chiral polyaniline, Helical structures, Electrodeposition, Binary doping

INTRODUCTION

Polyaniline (PAni) is one of the most interesting conducting polymers due to its excellent electrical, optical, and chemical properties, which makes it suitable for use in a wide range of technological applications.[1-4] Recently, much attention has been focused on chiral PAni because of its potential for use in several applications such as chiral separation, asymmetric electrochemical synthesis, electrochemical and biological sensors, and novel chiral molecular devices.[5,6] Because PAni does not have asymmetric carbon atoms on its backbone, its induced optical activity implies the existence of helical chirality.[7] The helical conformation of PAni is generally induced by using (+)-camphorsulfonic acid (CSA) or (-)-CSA as a chiral dopant. As CSA is a bidental dopant, chirality induction results from electrostatic interactions between the sulfonate anion in CSA and the radical cation $NH^{+\cdot}$ in aniline, and hydrogen bonding between the carbonyl group in CSA and the NH sites on the PAni chains.[8] The conformational changes induced in optically active conducting polymers have been of great interest because of their new opportunities for tuning the chiroptical properties of the polymers.[9,10] However, as the chiral conducting polymer is a type of rigid polymer, its conformational changes are not easy to be realized. There have been only a few reports regarding conformational changes in chiral PAni, which were induced by substitutions on the aniline ring, copolymerization, varying the solvent composition, or changing the polymerization temperature.[11-14] Moreover, these studies mostly involved chemical methods and there are few reports on the electrochemical polymerization of chiral PAni. To aim specifically at fabricating PAni-based devices to explore their potential applications, it is necessary to develop an electrochemical approach for the direct deposition of PAni onto electrodes in a simple and cost effective way. This could ensure a good ohmic contact between the electrode and the polymer.[15,16] In our previous study, by simply introducing a methoxy substituent at the ortho position of the phenyl ring, conformational changes in potentiodynamically deposited (+)-CSA-doped PAni (PAni-(+)-CSA) were observed.[17] In this study, the chiral dopant (+)-CSA was mixed with HCl in mole ratios of 9:1 (PAni-(9-1)) and 6:4 (PAni-(6-4)) to form a binary dopant for potentiodynamic deposition. Usually no obvious helical structure is observed directly in chiral PAni using microscopic techniques.[18] However, we were able to observe the helical structures of the deposited PAni films using scanning electron microscopy (SEM).[18] To our knowledge, there have been few reports on the conformational changes induced in chiral PAni through binary doping. The effects of the conformational changes on the crystallinity and morphology of the films were investigated by comparing their ultraviolet-visible (UV-Vis) and circular dichroism (CD) spectra and X-ray diffraction (XRD) patterns. The conductivity of the films was measured to observe the relationship between the helical ordering of polymer chain, crystallinity,

and conductivity.

EXPERIMENTAL

(+)- and (−)-CSA and dimethyl sulfoxide (DMSO) (ACS, reagent grade, 99.9%) were supplied by Sigma-Aldrich and used as received. Aniline monomer, HCl (37 wt%), ethanol, and acetone were purchased from Duksan Pure Chemicals. Aniline was purified by double distillation before use. All the solvents were obtained commercially and used without further purification, unless stated otherwise. All the aqueous solutions were prepared using deionized (DI) water. Aqueous solutions of the desired monomer (0.1 M) and of (+)- or (-)-CSA (0.1 M) were used as the supporting electrolytes. Prior to the experiments, nitrogen gas was flushed through the solutions to remove any dissolved oxygen as the oxygen dissolved in the solutions constitutes an electroactive species. and its reduction may interfere with the electrodeposition.[19] The electrochemical experiments were performed using a WBCS 3000 potentiostat (Won A Tech). An indium tin oxide (ITO) modified electrode was used as the working electrode with platinum plate (1.0 cm × 1.5 cm) counter and Ag/AgCl (3 M NaCl) electrode acting as reference electrodes. The ITO-coated glass substrates (sheet resistance of 9.55 Ω/sq) were rinsed with DI water and then ultrasonically cleaned in acetone for 15 min before the deposition process. The deposition area was 0.5 cm^2 and the rest of the substrate was covered with a layer of adhesive tape. The deposition was carried out in the potentiodynamic modes over the voltage range of 0.0 1.1 V at a scan rate of 10 mV/s over 40 cycles. The temperature of the electrolyte was maintained at 0 °C. The PAni-coated electrodes were dried in a vacuum oven at 60 °C for 24 h. The UV-Vis spectra were recorded with a S-3100 UV-Vis spectrophotometer (SCINCO) using DMSO as a solvent. Dedoped PAni in the emeraldine base form (PAni-EB) was obtained by dedoping PAni-(+)-CSA with NaOH. Fourier transform infrared (FT-IR) spectra were obtained using a FT-IR 4100 spectrometer (JASCO) with a PRO 470-H attenuated total reflection (ATR) single-reflection attachment. The CD spectra were recorded on a J-815 CD spectropolarimeter (JASCO) using DMSO as a solvent. Prior to the field-emission SEM (FE-SEM) imaging and conductivity measurements, the films were rinsed with ethanol to remove any unreacted monomer, possible oligomers, and unincorporated dopant. The surfaces of the films were Pt coated and then FE-SEM images were obtained at a magnification of 50k′ using a VEGA 3 LMU (TESCAN) system. The XRD patterns of the films were recorded on a D/Max-2200 X-ray diffractometer (RIGAKU) using Cu Kα radiation with the acceleration voltage of 40 kV and current of 40 mA. To measure the thicknesses of the films, an Alpha Step profilometer was used as a first approach. However, this technique failed because the soft polymer films were damaged by the metallic tip. Therefore, a Mitutoyo micrometer was employed for the thickness measurements. Conductivity measurements were taken using the four-point probe method with a 2401 source measurement unit (KEITHLEY).

RESULTS AND DISCUSSION

Cyclic Voltammetry

The electrochemical behavior and redox states of PAni are typically studied using cyclic voltammetry. In *Fig.* 1, the cyclic voltammograms (CVs) shows two main pairs of the reversible redox peaks. The first redox couple at lower positive potentials corresponds to the redox interconversion between leucoemeraldine base and emeraldine salt. The redox couple at the higher potential corresponds to the redox reaction between emeraldine salt and pernigraniline salt. As the films degraded with successive potential scans, the middle peak is observed between the two main oxidation peaks under certain conditions. The middle peak is most probably due to the redox couple of benzoquinone/hydroquinone, which is the main oxidized product of PAni.[6,20,21] During the potentiodynamic modes of deposition, an increase in the magnitude of the current suggests an increase in film thickness. The peak potential shifts regularly to more positive or negative values with

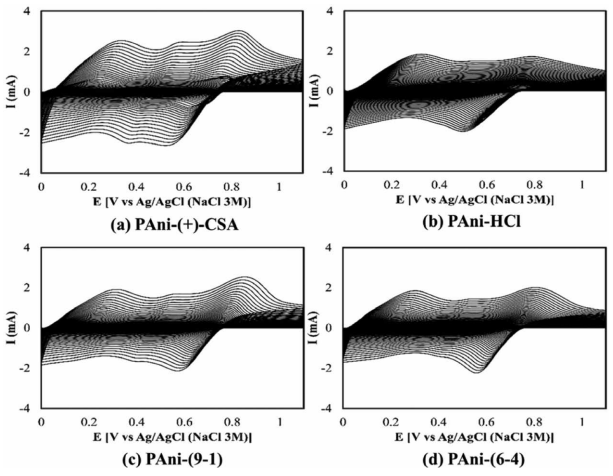

***Figure* 1.** CVs of the PAni films during electrodeposition: (a) PAni-(+)-CSA, (b) PAni-HCl, (c) PAni-(9-1), and (d) PAni-(6-4).

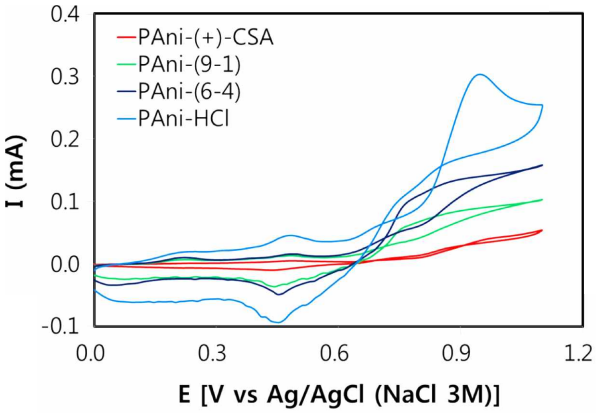

***Figure* 2.** CVs for the 3rd cycle for PAni-(−)-CSA, PAni-(9-1), PAni-(6-4), and PAni-HCl.

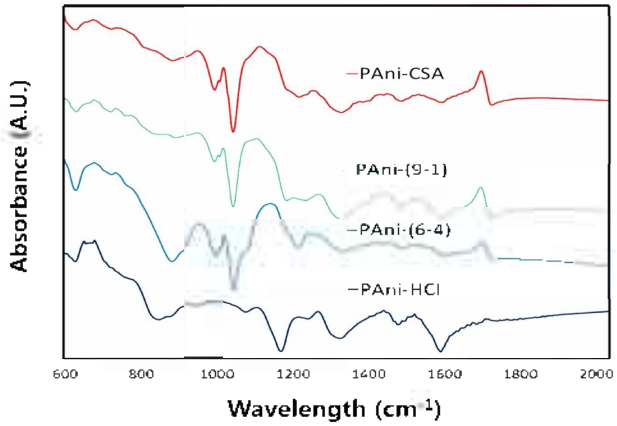

***Figure* 3.** FT-IR/ATR spectra of PAni-(+)-CSA, PAni-(9-1), PAni-(6-4), and PAni-HCl.

increasing thickness of the film due to the ohmic contribution to the overpotential.[19] The differences in the potentials and shapes of the peaks corresponding to binary-doped PAni and those for PAni-(+)-CSA and HCl-doped PAni (PAni-HCl), can be seen clearly in *Fig.* 1. Previous studies have suggested that the type of acid dopant used in the electrochemical polymerization is one of the main factors determining the electrochemical activity of the conducting polymer.[22] The CVs for the 3rd cycle, shown in *Fig.* 2, indicates that there are significant differences in the magnitudes of the peak current for the inversion potentials, depending on the type of dopant used. This result suggests that the dopants have a marked effect on the electrochemical behavior of PAni.

FT-IR Spectra

The characteristic FT-IR absorption peaks of PAni are shown in *Fig.* 3. The peak at ~1550 cm^{-1} arises mainly from the stretching of the C=N and C=C bonds of the quinoid ring (Q), while the peak at ~1480 cm^{-1} is attributed to the C-C stretching of the benzenoid ring (B). This implies that the polymer is composed of imine and amine units. The peak at ~1290 cm^{-1} is assigned to the stretching of the C-N bond of the secondary aromatic amine, while the peak at ~1140 cm^{-1} is assigned to the aromatic C-H in-plane bending and to the –NH^{+} stretching during the protonation process.[23–25] The above described peaks are observed in all samples, confirming the protonic acid doping of PAni. The peak at ~1000 cm^{-1}, corresponding to the out-of-plane bending vibrations of the C-H bond of the 1,4-disubstituted benzene ring, is indicative of the head-to-tail coupling of the aniline monomers during the polymerization.[26] The incorporation of CSA into PAni is confirmed by the peak at ~1730 cm^{-1} which is assigned to the C=O stretching vibrations of the $-SO_3$ group, and the peak at ~1030 cm^{-1} which is attributed to the –S=O stretching of the $-SO_3$ group.[27] The positions of the characteristic peaks of the binary-doped PAni and those of PAni-(+)-CSA are similar. The C-Cl stretching peak arises in the region at 600~700 cm^{-1}, which confirms the Cl^- doping of PAni. Thus, the obtained spectra confirm the expected structures of the polymer.

UV-Vis Spectra

The UV-Vis spectra of dedoped (PAni-EB) and protonic acid-doped PAni are shown in *Fig.* 4. PAni-EB exhibits two characteristic bands. The band at ~330 nm is assigned to the $\pi \rightarrow \pi^*$ transition in the benzenoid rings, which appears to be unaffected by doping with the protonic acids. Further, the band at ~630 nm could be assigned to the $n \rightarrow \pi^*$ transition (i.e., an exciton transition) due to the electron transition from a benzenoid to a quinoid ring.

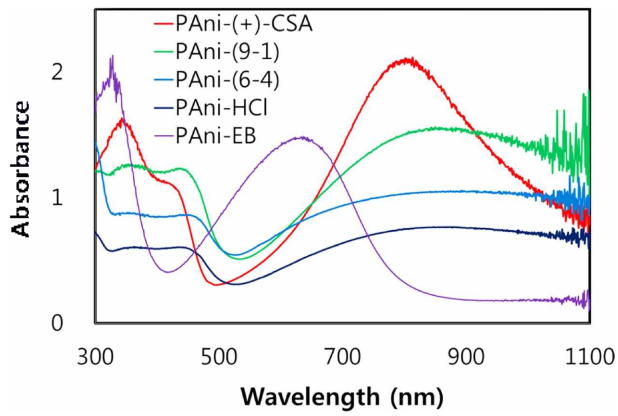

***Figure* 4.** UV-Vis spectra of PAni-(+)-CSA, PAni-(9-1), PAni-(6-4), PAni-HCl, and PAni-EB.

Similarly, the PAni doped with protonic acids exhibit three absorption bands: those related to the π →π* transition (at 300–340 nm), the polaron →π* transition (at ~440 nm), and the π→polaron transition (at ~850 nm).[28] The (+)-CSA doped PAni exhibits a characteristic broad shoulder that arises from the overlapping between the π→π* and polaron →π* transition bands and could be ascribed to the elimination of the band gap between the π and polaron bands.[29] The protonic acid doped PAni exhibits absorption bands with higher intensities at ~440 and ~850 nm. These polaronic transitions are indicative of the emergence of charge carriers, which is directly associated with the conductivity of the polymer.[30] PAni-(+)-CSA exhibits an intense, well-defined localized polaron band at ~850 nm which is considered as characteristics of the "compact coil" conformation of the PAni chains. However, the strong localized polaron band is weakened and broadened progressively as the fraction of (+)-CSA in the binary dopant mixture decreases, suggesting a partial release of the conformation of the polymer chain.[30] Thus, the absorption spectra of single- and binary-doped PAni are significantly different, indicating that conformational changes occurred in the polymer chains due to the binary doping.

CD Spectra

Fig. 5 shows the CD spectra of PAni doped with protonic acids. Since PAni does not have an asymmetric carbon atom in the structure, the induced optical activity as observed in the CD spectra implies the existence of a helical conformation.[7] PAni-(+)-CSA and PAni-(-)-CSA exhibit mirror image CD spectra of opposite sign, indicating the enantioselective induction of chirality in the PAni chains (*Fig.* 5, inset). The band due to the CSA^- ion (300 nm) and those attributable to the polymer backbone (330, 400, 455, and 750 nm) are indicative of the helical conformation of the polymer backbone. The bands at 330 and 400 nm are the bisignate, exciton-coupled bands associated with the benzenoid π→π* transition seen at 300–340 nm. Partly overlapping with these are another pair of bisignate, exciton-coupled CD bands at 400 and ~455 nm, these are associated with the polaron→π* transition observed at ~440 nm. The broad band centered at ~750 nm is associated with the localized polaron absorption band.[31] As PAni-(9-1) exhibits strong negative ellipticity at ~470 nm, the effect of the binary doping on the CD spectra is particularly interesting.[32] Thus, the conformation of polymer chains drastically changed compared to the PAni-(+)-CSA as the fraction of (+)-CSA decreased.[33] As observed in the UV-Vis spectra, PAni-(9-1) undergoes a partial release of the polymer chains. Nevertheless, its CD spectrum indicates that the majority of the polymer chains are still in the "compact coil" conformation.[11] From the UV and CD spectra, the association of the binary dopants result in destabilizing steric interactions between the dopants. Therefore, the polymer chains cannot retain their initial conformation. This conformational change diminishes its instability and produce a more stable polymer structure.[32]

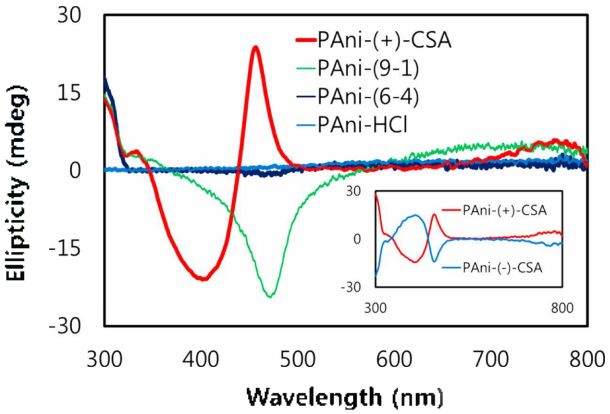

***Figure* 5.** CD spectra of PAni-(+)-CSA, PAni-(9-1), PAni-(6-4), and PAni-HCl.

SEM

Due to the progressive nucleation in the potentiodynamic modes, the deposited films exhibit smooth surface, uniform distributions, and good adhesion to the ITO electrode surface. Previous reports have shown that the interaction between (+)-CSA and PAni results in a left handed helical conformation as an evidence by the intense Cotton effects observed in the case of PAni-(−)-CSA.[11] It is well known that the direct observation of the helical structures using SEM is difficult but challenging, even for large biomolecules.[34] Nevertheless, it is very exciting that the helical structures of polymers in PAni-(+)-CSA and PAni-(9-1) can be observed using SEM (*Figs.* 6a, c). In keeping with the CD results, PAni-HCl shows an interconnected fibrillar morphology without the helical structure (*Fig.* 6b). The SEM images confirm that the polymer structure became relatively coiled when a small sized dopant such as HCl is used. However, the polymer exhibits a more swollen and expanded structure when it is doped with a bulky dopant such as CSA, resulting in a higher structural disorder.[35]

XRD

As can be seen from *Fig.* 7, the XRD pattern of (+)-CSA-doped PAni exhibits sharp and well-defined peaks, indicating that chiral (−)-CSA causes the remarkable increase

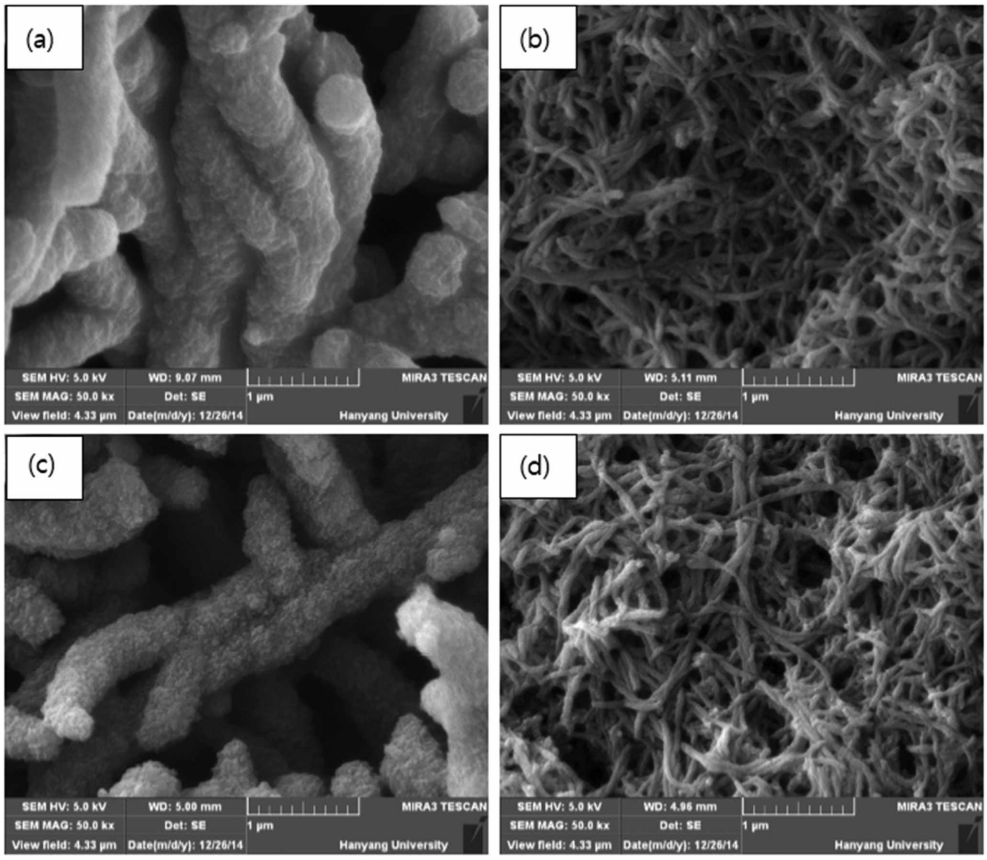

***Figure* 6.** SEM images of (a) PAni-(+)-CSA, (b) PAni-HCl, (c) PAni-(9-1), and (d) PAni-(6-4).

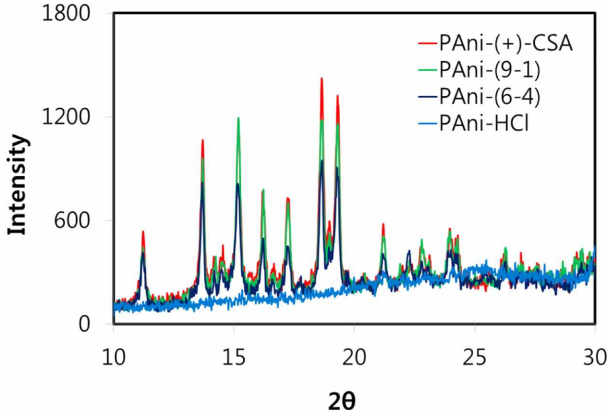

***Figure* 7.** XRD patterns of PAni-(+)-CSA, PAni-(9-1), PAni-(6-4), and PAni-HCl.

in the crystallinity due to the high degree of helical ordering. This is strongly supported by the helical structures seen in the SEM images of PAni-(−)-CSA and PAni-(9-1). The overall similarity in the diffraction patterns suggests that the films of PAni-(+)-CSA and binary-doped PAni have that basically the same structural arrangement. However, PAni-HCl does not show any well-defined peaks. This suggests that it has an amorphous structure. The peaks at 2θ of 11.2°, 13.7°, 18.6°, and 19.3 are attributed to (−)-CSA, while those at 15.2°, 21.2°, and ~26.3° are related to the crystal structure of PAni. The peak at 15.2° is related to the intrachain ordering within the PAni molecules. The increase in the intensity of the peak at 21.2° in the case of PAni-(+)-CSA implies improved π-π interchain stacking.[17] It is expected that the highly ordered structure improves the crystallinity, resulting in increased conductivity because of the enhancement of carrier mobility in the films.

Conductivity

In this study, we are interested in studying the effects of structural and morphological changes on the conductivity of PAni. The total conductivity of a conducting polymer depends on both the ability of its charge carriers to move along the polymer backbone (intrachain charge transfer) and the ability of the charge carriers to hop between the polymer chains (interchain charge transfer).[36] It is observed that the conductivity increases with increasing mole fraction of (−)-CSA: PAni-(+)-CSA (4.55 S cm^{-1}), PAni-(9-1) (4.31 S cm^{-1}), PAni-(6-4) (1.61 S cm^{-1}), and PAni-HCl (0.80 S

cm^{-1}). The increased conductivity of PAni-(+)-CSA and PAni-(9-1) seems to be closely related to the improvement in the intrachain charge carrier mobility along the helical polymer backbone. The intrachain mobility in the PAni films is strongly influenced by the chain structure in the films, as evidenced by the previously discussed CD and SEM results. As the chiral dopant (+)-CSA induces a predominantly one-handed helical ordering of the polymer backbone, this trend in the conductivity is also consistent with the obtained XRD results. The highly ordered structure improves the crystallinity, resulting in increased charge carrier mobility through the increased interchain charge transfer. As expected, PAni-HCl exhibits a lower conductivity than the (+)-CSA-doped PAni due to the typical amorphous structure of the former.

CONCLUSION

PAni films doped with a binary dopant ((+)-CSA/HCl) were prepared by potentiodynamic deposition. Considerable changes are induced by the binary doping in the chiroptical properties and conformation of chiral PAni. The helical structures in PAni-(+)-CSA and PAni-(9-1) can be observed using SEM. The remarkable increase in crystallinity is observed in the case of (+)-CSA-doped PAni due to the helical ordering induced by the chiral dopant. Consequently, the increase in interchain and intrachain charge transfer result in a higher conductivity in the case of PAni-(+)-CSA. Further, the interrelationship between the helical ordering of polymer chain, crystallinity, and conductivity are observed.

Acknowledgments. Publication cost of this paper was supported by the Korean Chemical Society.

REFERENCES

1. Ćirić-Marjanović, G. *Synth. Met.* **2013**, *177*, 1.
2. Sajeev, U. S.; Nambuthiri, V. V.; Salah, A.; Nampoori, V. P. N.; Anantharaman, M. R. *Synth. Met.* **2010**, *160*, 1704.
3. Bejbouji, H.; Vignau, L.; Miane, J. L.; Dang, M. T.; Oualim, E. M.; Harmouchi, M.; Mouhsen, A. *Sol. Energ. Mat. Sol. C* **2010**, *94*, 176.
4. Anjum, M. N.; Zhu, L.; Luo, Z.; Yan, J.; Tang, H. *Polymer* **2011**, *52*, 5795.
5. Weng, S. H.; Zhou, J. Z.; Lin, Z. H.; Lin, X. H. *Chem. J. Chinese U* **2012**, *33*, 2501.
6. Pornputtkul, Y.; Kane-Maguire, L. A. P.; Innis, P. C.; Wallace, G. G. *Chem. Commun.* **2005**, *36*, 4539.
7. McCarthy, P. A.; Huang, J.; Yang, S. C.; Wang, H. L. *Langmuir* **2002**, *18*, 259.
8. Kane-Maguire, L. A. P.; Wallace, G. G. *Chem. Soc. Rev.* **2010**, *39*, 2545.
9. Yan, Y.; Deng, K.; Yu, Z.; Wei, Z. X. *Angew. Chem., Int. Ed.* **2009**, *48*, 2003.
10. Leiras, S.; Freire, F.; Seco, J. M.; Quiñoá, E.; Riguera, R. *Chem. Sci.* **2013**, *4*, 2735.
11. Yan, Y.; Fang, J.; Liang, J.; Zhang, Y.; Wei, Z. *Chem. Commun.* **2012**, *48*, 2843.
12. Su, S. J.; Takeishi, M.; Kuramoto, N. *Macromolecules* **2002**, *35*, 5752.
13. Egan, V.; Bernstein, R.; Hohmann, L.; Tran, T.; Kaner, R. B. *Chem. Commun.* **2001**, *37*, 801.
14. Pornputtkul, Y.; Kane-Maguire, L. A. P.; Wallace, G. G. *Macromolecules* **2006**, *39*, 5604.
15. Weng, S.; Lin, Z.; Chen, L.; Zhou, J. *Electrochim. Acta* **2010**, *55*, 2727.
16. Qin, Q.; Guo, Y. *J. Nanomater.* **2012**, *2012*, 1.
17. Lee, E.; Kim, E. *Bull. Korean Chem. Soc.* **2013**, *34*, 1.
18. Xu, L.; Chen, Z.; Chen, W.; Mulchandani, A.; Yan, Y. *Macromol. Rapid Commun.* **2008**, *29*, 832.
19. Atassi, Y.; Tally, M. *ArXiv Preprint ArXiv*: 1307.5668, **2013**, 1.
20. Somerset, V.; Leaner, J.; Mason, R.; Iwuoha, E.; Morrin, A. *Electrochim. Acta* **2010**, *55*, 4240.
21. Gu, J.; Kan, S.; Shen, Q.; Kan, J. *J. Electrochem. Sci.* **2014**, *9*, 6858.
22. Fenelon, A. M.; Breslin, C. B. *Synth. Met.* **2004**, *144*, 125.
23. Du, X.; Xu, Y.; Xiong, L.; Bai, Y.; Zhu, J.; Mao, S. *J. Appl. Polym. Sci.* **2014**, *131*, 40827.
24. Zamora, P. P.; Díaz, F. R.; del Valle, M. A.; Louarn, G.; Cattin, L.; Bernède, J. C. *Int. J. Sci.* **2013**, *2*, 1.
25. Abdiryim, T.; Xiao-Gang, Z.; Jamal, R. *Mater. Chem. Phys.* **2005**, *90*, 367.
26. Morsi, R. E.; Khamis, E. A. *Int. J. Sci. Res.* **2014**, *3*, 1317.
27. Osorio-Fuente, J. E.; Gómez-Yáñez, C.; Hernández-Pérez, M. A.; Pérez-Moreno, F. *J. Mex. Chem. Soc.* **2014**, *58*, 52.
28. Sharma, S.; Kumar, D. *Indian J. Eng. Mater. Sci.* **2010**, *17*, 231.
29. Kang, M.; Lee, J. E.; Shim, H. W.; Jeong, M. S.; Im, W. B.; Yoon, H. *RSC Adv.* **2014**, *4*, 27939.
30. Innis, P. C.; Norris, I. D.; Kane-Maguire, L. A. P.; Wallace, G. G. *Macromolecules* **1998**, *31*, 6521.
31. McCarthy, P. A.; Huang, J.; Yang, S. C.; Wang, H. L. *Langmuir* **2002**, *18*, 259.
32. Norris, I. D.; Kane-Maguire, L. A. P.; Wallace, G. G. *Macromolecules* **2000**, *33*, 3237.
33. Yuan, G. L.; Kuramoto, N. *Macromolecules* **2002**, *35*, 9773.
34. Yashima, E. *Polym. J.* **2010**, *42*, 3.
35. Wang, Y.; Tran, H. D.; Liao, L.; Duan, X.; Kaner, R. B. *J. Am. Chem. Soc.* **2010**, *132*, 10365.
36. Lee, J.; Kim, E. *Bull. Korean Chem. Soc.* **2011**, *32*, 2661.